Variations in vertical CO/CO_2 profiles in the Martian mesosphere and lower thermosphere measured by ExoMars TGO/NOMAD: Implications of variations in eddy diffusion coefficient

N. Yoshida, *Graduate School of Science, Tohoku University, Sendai, Japan* (nao.yoshida.q7@dc.tohoku.ac.jp), **H. Nakagawa**, *Graduate School of Science, Tohoku University, Sendai, Japan*, **S. Aoki**, *Graduate School of Frontier Sciences, The University of Tokyo, Kashiwa, Japan*, **J. Erwin**, *Royal Belgian Institute for Space Aeronomy, BIRA-IASB, Brussels, Belgium*, **A. C. Vandaele**, *Royal Belgian Institute for Space Aeronomy, BIRA-IASB, Brussels, Belgium*, **F. Daerden**, *Royal Belgian Institute for Space Aeronomy, BIRA-IASB, Brussels, Belgium*, **I. Thomas**, *Royal Belgian Institute for Space Aeronomy, BIRA-IASB, Brussels, Belgium*, **L. Trompet**, *Royal Belgian Institute for Space Aeronomy, BIRA-IASB, Brussels, Belgium*, **S. Koyama**, *Graduate School of Science, Tohoku University, Sendai, Japan*, **N. Terada**, *Graduate School of Science, Tohoku University, Sendai, Japan*, **L. Neary**, *Royal Belgian Institute for Space Aeronomy, BIRA-IASB, Brussels, Belgium*, **I. Murata**, *Graduate School of Science, Tohoku University, Sendai, Japan*, **G. Villanueva**, *NASA Goddard Space Flight Center, MD, USA*, **G. Liuzzi**, *NASA Goddard Space Flight Center, MD, USA*, **M. A. Lopez-Valverde**, *Instituto de Astrofisica de Andalucia (IAA/CSIC), Granada, Spain*, **A. Brines**, *Instituto de Astrofisica de Andalucia (IAA/CSIC), Granada, Spain*, **A. Modak**, *Instituto de Astrofisica de Andalucia (IAA/CSIC), Granada, Spain*, **Y. Kasaba**, *Graduate School of Science, Tohoku University, Sendai, Japan*, **B. Ristic**, *Royal Belgian Institute for Space Aeronomy, BIRA-IASB, Brussels, Belgium* **G. Bellucci**, *Institute di Astrofisica e Planetologia Spaziali (IAPS/INAF), Rome, Italy*, **J. J. López-Moreno**, *Instituto de Astrofisica de Andalucia (IAA/CSIC), Granada, Spain*, and **M. Patel**, *School of Physical Sciences, The Open University, UK*

Introduction:

CO is produced by the photodissociation of CO_2 and recycled to CO_2 by the catalytic cycle involving HOx in the Martian atmosphere [e.g., McElroy & Donahue, 1972]. The photochemical lifetime of CO is ~6 years in the lower atmosphere [Krasnopolsky, 2007]. While, in the middle and upper atmosphere (> ~50 km), the photochemical lifetime of CO becomes even much longer due to the decrease in the HOx species density and longer than the characteristic times of production and eddy diffusion. It suggests that CO profiles are determined by the production and eddy diffusion at those regions. The eddy diffusion coefficient is used for parameterizing the efficiency of vertical diffusion, however, estimated values have a large scatter between 40 and 90 km altitude [Rodrigo et al., 1990]. Recently, a substantial variation in the eddy diffusion coefficient at the homopause altitude has been suggested [Slipski et al., 2018]. It implies that CO profiles in the middle and upper atmosphere vary with variations in the eddy diffusion coefficient. ExoMars Trace Gas Orbiter (TGO) can measure the vertical profiles of CO in the mesosphere and thermosphere. Olsen et al. (2021) reported the vertical distribution of CO and its variation during a dust storm, however, the effects of change in the eddy diffusion coefficient on the profile of CO mixing ratio have not been investigated. In this study, we use Nadir and Occultation for MArs Discovery (NOMAD, Vandaele et al., 2018) aboard TGO to retrieve the vertical CO/CO_2 profile and to investigate the variability of the eddy diffusion coefficient.

Dataset and analysis:

Here, we applied the equivalent width technique [Chamberlain & Hunten, 1987; Krasnopolsky, 1986] to derive CO and CO_2 column densities. In the case that the optical depth of the absorption line is not saturated, the slant column density is given by $W = SN$, where W is the area of absorption, S is the line intensity, and N is the slant column density in the line of sight. We derived the slant column density using 4288.2 and 4291.5 cm^{-1} for CO and 3355.7, 3357.2, 3358.7, and 3360.3 cm^{-1} for CO_2. The CO/CO_2 ratio is derived between 70 and ~105 km altitudes. We use only the orbits which measure CO spectra (in order 190, 4269.95 – 4303.99 cm^{-1}) and CO_2 spectra (in order 149, 3348.54 – 3375.23 cm^{-1}) simultaneously in MY 35, corresponding from 25th March 2019 to 6th February 2021. The total number of orbits used in this study is 649.

Results and discussion:

We found that the retrieved CO/CO_2 ratio between 70 and ~105 km shows a significant seasonal variation in the southern hemisphere, which decreases near perihelion and increases near aphelion between ~1500 and ~5000 ppm at 85 km. The slope of CO/CO_2 profiles becomes steep near perihelion in the southern hemisphere (**Figure 1**). To investigate the contribution of the variability of the eddy diffusion coefficient in each hemisphere and season, we estimated the best CO/CO_2 profile by a 1D photochemical model [Koyama et al., 2021] using a chi-square test with two cases: (1) the eddy diffusion coefficients are uniform in vertical; (2) the vertical profile of eddy diffusion coefficient is given by $K = An^{-1/2}$, where A is constant, and n is total number density [cf. Lindzen, 1971]. Our estimation shows that the altitude-dependent eddy diffusion coefficient is better than the vertically-uniform eddy diffusion coefficients to reproduce the observed profiles (**Figure 2**). In addition, our observation firstly suggested the variation of the eddy diffusion coefficient. In the southern hemisphere, $K = 4.25\times10^{13}n^{-1/2}$ for L_s = 90 – 120 and $K = 1.5\times10^{14}n^{-1/2}$ for 240 – 270. Throughout the altitude range, the eddy diffusion coefficient in L_s = 240 – 270 is larger by a factor of ~2 than that in L_s = 90 – 120 in the southern hemisphere. On the other hand, the estimated eddy diffusion coefficient in the northern hemisphere is comparable between both L_s ranges; $K = 7\times10^{13}n^{-1/2}$ for L_s = 90 – 120 and $K = 10^{14}n^{-1/2}$ for 240 – 270. That would suggest the efficiency of the vertical diffusion varies with season and latitude.

Figures:

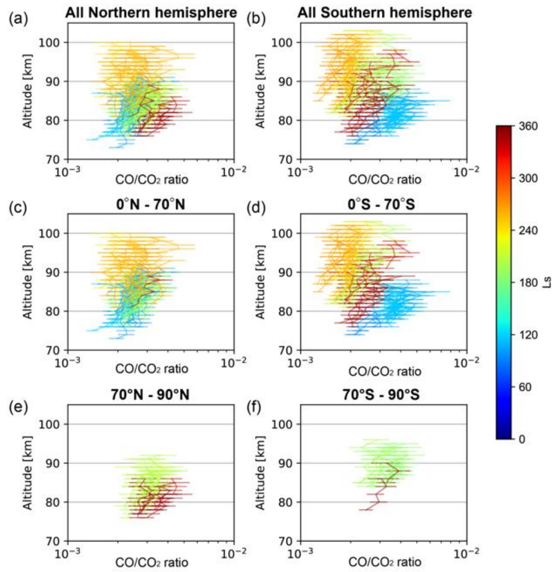

Figure 1 Vertical profiles of the CO/CO_2 ratio in L_s = 90 – 120, 180 – 210, 240 – 270, and 330 – 360 in MY 35. Horizontal lines are error bars. Color represents L_s. Profiles are separated into the northern (a, c, and e) and southern (b, d, and f) hemispheres. To distinguish the enhancement in polar regions, profiles are separated into two latitudinal bins: from the equator to 70 degrees (c and d) and 70 to 90 degrees (e and f).

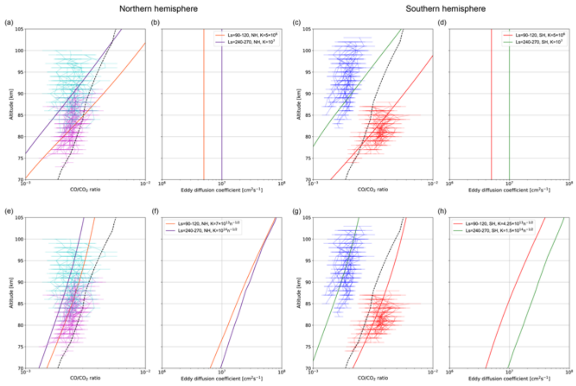

Figure 2 (a, c, e, and g) Vertical profiles of the CO/CO_2 ratio estimated with the 1D model and observed by NOMAD SO. The broken lines represent the initial CO/CO_2 profiles in the model. For the northern (southern) hemisphere, the observed CO/CO_2 profiles in L_s = 240 – 270 is shown in light blue (blue), and that in L_s = 90 – 120 is in magenta (red). (b, d, f, and h) The determined eddy diffusion coefficients used for the 1D model. L_s are distinguished by colors. Profiles are divided into two hemispheres, those in the northern hemisphere are shown in panels (a, b, e, and f), and those in the southern hemisphere in panels (c, d, g, and h).

Bibliography:

Chamberlain & Hunten (1987), Theory of planetary atmospheres: an introduction to their physics and chemistry. *Academic Press.*

Krasnopolsky (1986), Photochemistry of the atmospheres of Mars and Venus. Physics and Chemistry in Space 13. *Springer*.

Krasnopolsky (2007), Long-term spectroscopic observations of Mars using IRTF/CSHELL: mapping of O_2 dayglow, CO, and search for CH_4. *Icarus, 190*, 93-102. doi:10.1016/j.icarus.2007.02.014.

Lindzen (1971), Tides and gravity waves in the upper atmosphere. *Mesospheric Models and Related Experiments*, 122-130.

McElroy & Donahue (1972), Stability of the Martian atmosphere. *Science, 177 (4053)*, 986-988. DOI:10.1126/science.177.4053.986.

Olsen et al. (2021), The vertical structure of CO in the Martian atmosphere from the ExoMars Trace Gas Orbiter. *Nature geoscience*, https://doi.org/10.1038/s41561-020-00678-w.

Rodrigo et al. (1990), A nonsteady one-dimensional theroretical model of Mars' neutral atmospheric composition between 30 and 200 km. *Journal of Geophysical Research, vol. 95*, No. B9, 14795-14810. 90JB00158.

Slipski et al. (2018), Variability of Martian turbopause altitudes. *Journal of Geophysical Research: Planets*, *123*, 2939-2957. https://doi.org/10.1029/2018JE005704.

Vandaele et al. (2018), NOMAD, an integrated suite of three spectrometers for the ExoMars Trace Gas Mission: Technical description, science obsectives and expected performance. *Space Science Review*, *214*:80. https://doi.org/10.1007/s11214-08-0517-2.